

Design considerations for valve dynamics of a positive displacement cryogenic pump

Luke Humphreys^{1*} and Brandon Demski¹

¹ P3 Technologies, Jupiter, USA

*E-mail: Luke.Humphreys@p3-tech.com

**E-mail: Brandon.Demski@p3-tech.com

Abstract. Operation of a cryogenic pump near saturated conditions proves challenging to maintain fluid quality throughout the intake process of the pump. Design considerations for minimizing the phase change of fluid across the pump are explored, highlighting the goal of maximizing mass flow throughput of the positive displacement pump. CFD studies were conducted to predict state change performance across the inlet valve of the pump in saturated liquid nitrogen conditions. High-speed video of the designed valve operating in liquid nitrogen on an optically accessible cryogenic setup were captured to validate the CFD predictions. Experimental results indicate good agreement with qualitative CFD analysis regarding state change performance, and demonstrate the underlying dynamics of designing dynamic cryogenic valves.

1. Introduction and background

Positive Displacement (PD) pumps excel in many difficult parameter spaces are particularly advantageous in the low-flowrate, high pressure operating corner [1]. This operating corner is highly prevalent in cryogenic spaceflight applications and is becoming more prevalent in cryogenic terrestrial applications such as in the medical industry [2–4]. In spaceflight applications, the majority of work in PD cryogenic pumps focuses on low pressures due to the various design challenges inherent in higher output pressures and limited application scope [5–8]. In terrestrial applications, cryogenic PD pump development has focused on larger scale distribution of cryogenic fluids, such as in LNG and industrial liquid hydrogen facilities [9–11]. Thus, there exists opportunity for research and innovation in the design space for low-flowrate, high pressure cryogenic positive displacement pump regime.

There is increasing interest in the storage and distribution of cryogenic propellants and other fluids in spaceflight applications in larger quantities and more varied applications[12]. Storing propellants as cryogenic liquids allows for high density storage of propellants at low tank pressures, which helps reduce tank structural requirements, minimizing propellant tank mass. These considerations, combined with the increasing scope and duration of space missions, leads to cryogenic fluid management becoming an increasingly important realm of space exploration [13]. Due to the advantages of positive displacement pumps in energy efficiency, they are particularly attractive for meeting the demand of these spaceflight applications.

Often in cryogenic applications, the storage tanks of fluids are maintained at saturated conditions due to the various costs of maintaining subcooling overhead. Thus, it is important to consider operation of cryogenic pumps at or near zero Net Positive Suction Pressure (NPSP)



conditions. Cryogenic PD pump design presents significant challenges to optimizing valve geometries to minimize the fluid density shift across the valve during the intake stroke to maintain the required flowrate of the pump. Previous work has been conducted investigating the valve performance of PD pumps, especially computationally, but is generally limited to much larger systems [14–16].

This investigation seeks to provide a framework for the design and computational analysis of a positive displacement valve, demonstrating common considerations for the valve design across a variety of cryogenic propellants desirable for spaceflight applications. An electro-kinetic model is used to predict the valve kinematics, along with a CFD model predicting the fluid density throughout the intake stroke. In addition, experimental measurements for both quantitative and qualitative properties of the valve are used to help validate the computational analysis.

2. Test design and setup

2.1 Kinematic modelling

To understand the kinematic motion of the system due to the lift generated by the valve from the differential pressure needs to be quantified. This lift is generated due restrictive area of the valve and the valve seat creating an orifice, forcing a pressure drop across the valve whenever a pressure differential is generated. The position of the valve will have a strict determination of the lifting coefficients and in turn the acceleration potential of the system. These effects are further exacerbated by the two-phase effects incurred when operating at zero-NPSP, where any increase in velocity or decrease in pressure causes a degradation of density.

To evaluate the fluid dynamic effects on the valve transients, an ANSYS CFX model was setup evaluate the transient behaviour of the valve. These analyses were used to quantify the valve opening and closing times transiently to correlate the effects of the differential pressures on the valve and the corresponding lifting coefficients as a function of velocity and position. These analyses utilized two-phase fluid files to capture the effects of the phase change in a plurality of cryogens, such as liquid hydrogen, nitrogen, and oxygen. The transient CFD model was compared against predictive methodologies that utilized a time transient calculation in excel using variable predictive lift coefficients and a fourth order Runge-Kutta methodology.

2.2 Experimental design setup

To better understand the performance of the cryogenic valve, an optically accessible test rig was designed and constructed to both quantitatively and qualitatively examine the performance of the designed cryogenic valve. Photographs of the valve insert, along with the test apparatus with insert installed are shown in Figure 1.

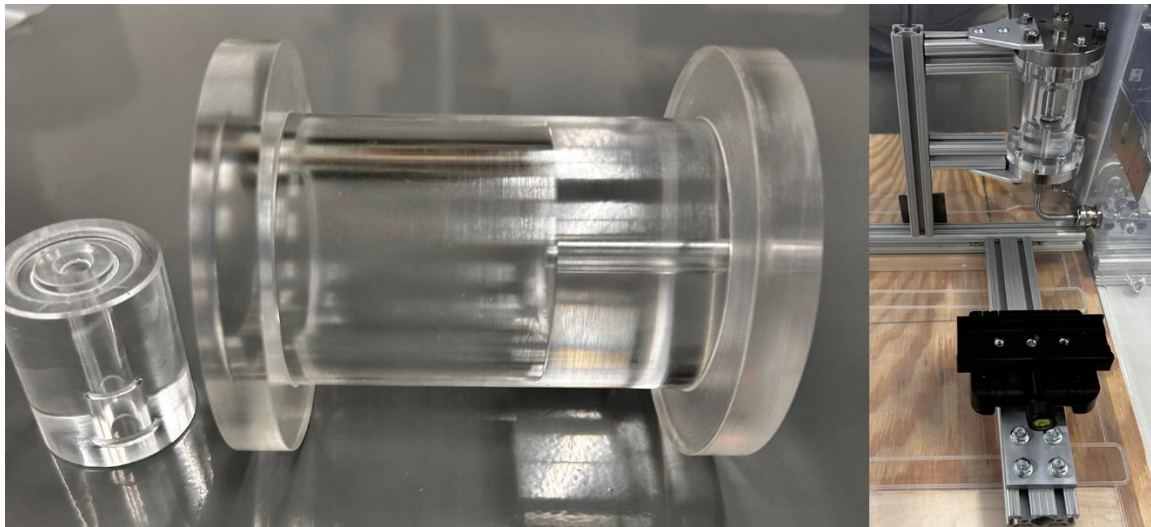


Figure 1. Photograph of optically accessible valve cycling apparatus mounted in test configuration (right), with ball and conic valve insert shown separately (left)

High speed images were taken of the valve during a simulated intake stroke, which was opened and closed via two remotely operated solenoid valves, which was synchronized with a high speed camera system to observe the fluid dynamics surrounding the valve during operation. While the target application and CFD studies were conducted across a variety of cryogenic propellants, this initial experimental investigation limited its scope to liquid nitrogen to mitigate the hazards of working with non-inert gases. Liquid nitrogen was supplied from a cryogenic dewar through a remotely operated valve. A Chronos 1.4 high speed camera was utilized to capture high speed image series of the ball actuating. The high speed camera was mounted in position across from the clear valve body design, and the intake stroke of the pump was simulated by opening and closing the upstream and downstream ROV's alternately. This assembly was then enclosed in a chamber which was positively pressurized with industrially pure dry nitrogen to prevent condensation from forming on the clear valve body during cryogenic operation.

The valve geometry tested was a 0.25 inch [6.35mm] silicon nitride ball, set into a matching conic valve seat, machined from PTFE. Primary concerns for material selection of the valve poppet and seat were cryogenic propellant compatibility, including liquid oxygen and liquid hydrogen, material strength, as well as thermal expansion considerations in the optically accessible test rig. Silicon nitride balls have seen extensive use in demanding cryogenic applications such as bearings in high speed turbopumps [17]. PTFE was chosen for the valve seat to remain physically constrained during the substantial temperature gradient experienced during cryogenic chill-in in the acrylic housing.

Testing was conducted by opening the two ROV's at a frequency of 3 Hz to actuate the valve several times during the camera capture, providing enough dwell time duty cycle to ensure that the full valve cycle time would not be truncated due to insufficient dwell time. In practice, this dwell time should be optimized for each valve based upon the performance requirements of the pump and is measurable for such an optimization effort in the test setup.

3. Results and discussion

3.1 Valve CFD and kinematics modelling results

Using the pressure gradient on the valve, shown in the left side of Figure 2 the valve lifting coefficients were evaluated and extracted as a function of position and velocity from the CFD analyses to create the second order function required to predict valve timing performance. This equation was used to develop the overall governing kinematic equation of motion for this valve geometry utilizing the varying cryogenic fluids at their respective thermodynamic states. Through the RK4 integration calculations, the effective valve kinematics were able to be assessed.

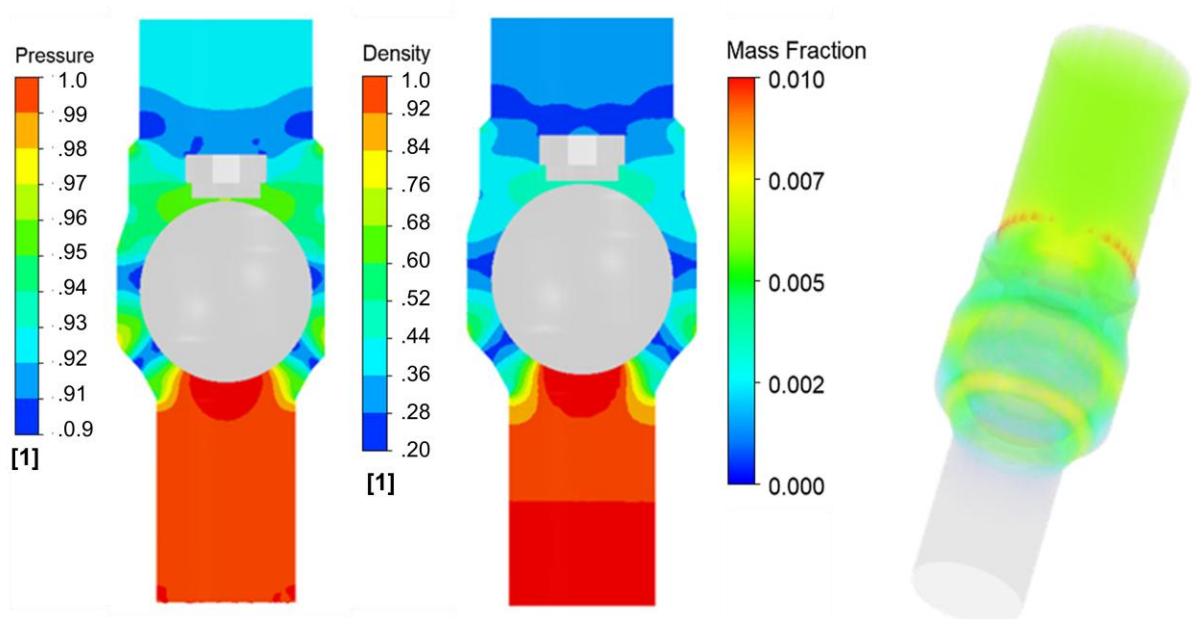


Figure 2. CFD Results showing pressure and density predictions for the low NPSP test case, along with two phase mass fraction

In addition, the density gradient across the valve is calculated throughout the flow field and is shown on the central image of Figure 2. When operating near NPSP, this sudden pressure drop results in a large reduction in density due to the phase transition of the fluid in these low-pressure regions. This results in a large degradation in the mass fraction of the fluid entering the compression volume, resulting in significant degradation in flow rate. Optimizing the valve to minimize this pressure drop across the valve is critical in improving the performance of a PD cryogenic pump when operating near saturated liquid conditions.

3.2 Valve timing experimental validation

The valve timing predictions were then measured experimentally using the optically accessible test rig described above. The valve was cycled while images were taken by the high-speed camera at a frame rate of 5000 frames per second. Figure 3 shows a representative image series from the high NPSP cycling without the travel stop installed showing the valve opening actuation.

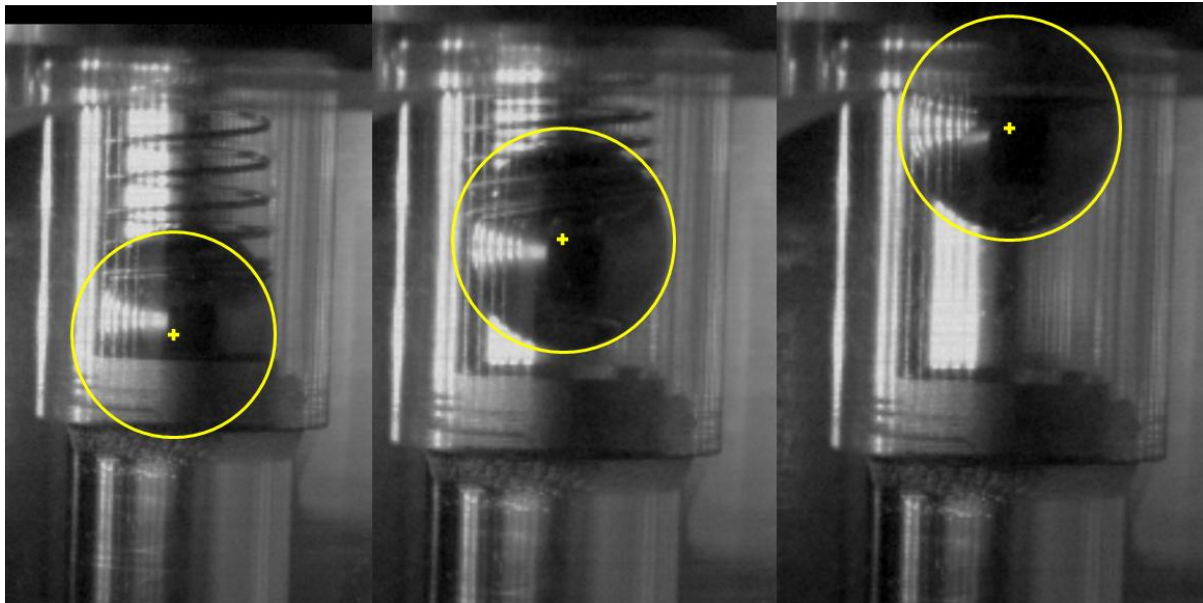


Figure 3. Representative image series showing valve opening during high NPSP cycling without travel stops implemented, and calculated ball position overlaid onto image

The images are then processed using Octave, utilizing a Hough transformation algorithm to determine the ball position for each frame. The algorithm utilized is not particularly robust without sufficient image pre-processing resulting in some false measurements during images with high optical occlusion, but the data is sufficiently resolved to determine opening and closing times. Figure 4 shows the calculated ball position during 1 second of operation in the High NPSP cycling operation case, showing the valve cycling at the 3 Hz operational frequency.

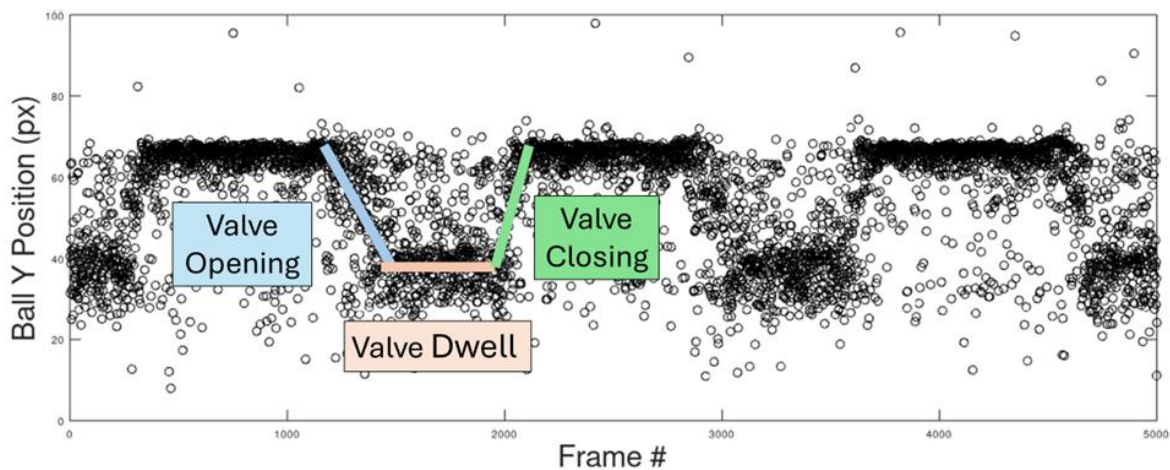


Figure 4. Calculated valve Y-position vs. frame number during high NPSP cycling

From this data, the valve opening time, dwell time, and valve closing time can be determined. The raw data is processed to help further reduce outliers in the positioning determination, and then a linear interpolation is taken to estimate the intercept with the two dwell regions. This allows for computation of the various valve cycling times for each of the three captured valve cycles and is then averaged across the three cycles. The calculated valve opening and closing times for the two-test series are shown in Table 1 below, compared with the calculated opening times predicted from the analytical modelling.

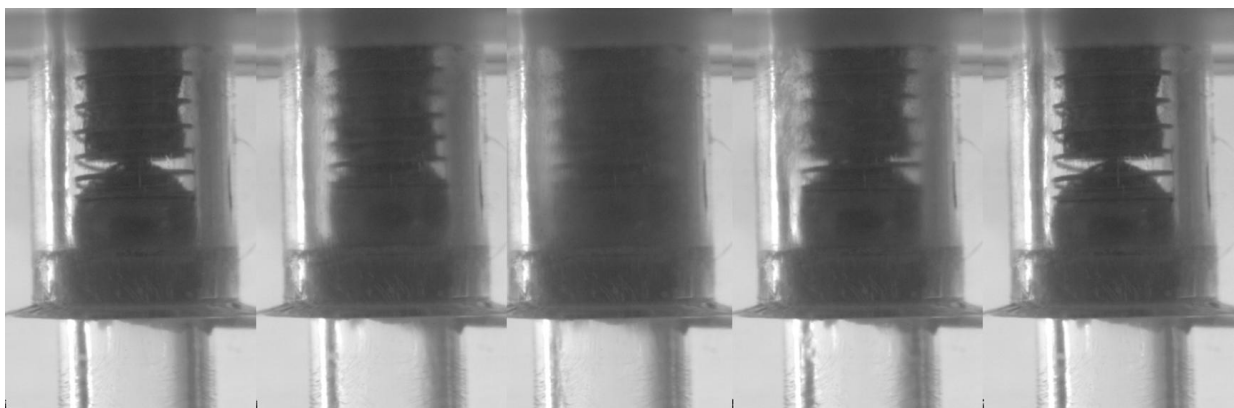
Table 1. Experimentally determined and analytically computed valve opening and closing times for each

Test Series	Experimental Valve Opening Time	Analytical Valve Opening Time	Experimental Valve Closing Time	Analytical Valve Closing Time
High NPSP Testing	11 ms	13 ms	6 ms	6 ms
Low NPSP Testing	40 ms	41 ms	25 ms	27 ms

There is some significant hysteresis between the valve opening and closing times, which is attributed to the vertical testing orientation of the valve. The addition of gravitational force on the ball working against the fluid pressure during the valve opening cycle increases the time required to open the valve. Similarly, the weight works towards helping the valve close, resulting in a faster closing time than opening time. The predicted analytical results match well with the experimentally determined data. This modelling can then be further refined by employing a tuning parameter built into the drag coefficient of the valve geometry based upon further experimental validation to produce even higher fidelity performance predictions of the valve.

3.3 Fluid density shift computational modelling and experimental validation

The low NPSP test case is particularly interesting from a fluid density shift perspective. Since there is low thermal margin between phase states, the sudden decrease in pressure acting around the valve causes some of the liquid cryogen to transition to gas, which can be seen in the regions of optical occlusion as shown in Figure 5, which shows an image series showing a full actuation cycle, with the valve opening and closing.

**Figure 5.** High Speed Image series of low NPSP testing showing valve opening and closing and phase transition of liquid nitrogen around valve

The central image, which shows the valve fully open, shows how the region immediately surrounding the ball is the most optically occluded. The optical occlusion occurs due to the mismatch in refractive index between the gas bubbles formed due to gaseous nitrogen in the fluid, and thus represents the areas with the least mass fraction. This agrees qualitatively with the CFD predictions, showing two rings of low mass fraction in the low pressure regions surrounding the

ball. Minimizing the pressure differential across the valve thus reduces the amount of vapor transition, which increases the delivered flowrate to the compression volume of the pump.

4. Conclusions and future work

A methodology for analysing valve performance is presented, highlighting the importance of valve design and kinematics. Experimental results show good agreement with computationally predicted performance, both in quantitative valve timing measurements, along with qualitative observation of the fluid.

Future work is intended to cover a broader range of operating conditions and valve geometries, providing further insight into general valve design considerations. Additionally, different valve and seat materials can be utilized, and flowrates can be measured to determine pump design parameters such as fluid intake flowrates.

References

- [1] American Institute of Chemical Engineers 2007 *Positive Displacement Pumps: A Guide to Performance Evaluation* (Hoboken: Wiley)
- [2] Erinjeri J P and Clark T W 2010 Cryoablation: mechanism of action and devices *Journal of Vascular and Interventional Radiology* **21**:S187 91
- [3] Collaudin B and Rando N 2000 Cryogenics in space: a review of the missions and of the technologies *Cryogenics* **40** 797–819 ([https://doi.org/10.1016/S0011-2275\(01\)00035-2](https://doi.org/10.1016/S0011-2275(01)00035-2))
- [4] Doherty M, Gaby J, Salerno L and Sutherlin S 2009 Cryogenic Fluid Management Technology for Moon and Mars Missions *AIAA SPACE 2009 Conference & Exposition*, American Institute of Aeronautics and Astronautics (<https://doi.org/10.2514/6.2009-6532>)
- [5] Darabi J and Wang H 2005 Development of an electrohydrodynamic injection micropump and its potential application in pumping fluids in cryogenic cooling systems *Journal of Microelectromechanical Systems* **2005**;14 747–55
- [6] Air Squared Inc. 2017 Spinning-Scroll Pump for Cryogenic Feed System *NASA Technical Report*
- [7] Jedrich N M *et al* 2003 Cryogenic cooling system for restoring IR science on the Hubble space telescope *SPIE* **4850** 1058–69
- [8] Zhang X, Zhao Y, Li B and Ludlow D 2004 Pumping capacity and reliability of cryogenic micro-pump for micro-satellite applications *Journal of Micromechanics and Microengineering* **2004**;14 1421
- [9] Gieras J F, Piech Z J and Tomczuk B 2018 *Linear synchronous motors: transportation and automation systems* (CRC press) (<https://doi.org/10.1201/b11105>)
- [10] Han S, Kim Y, Choi Y, Jo S, Maletzko A and Hwang J 2024 Development of Technical Specifications and Process System Requirements for the World's Largest LH2 Refueling Station *EDP Sciences* **521** 01003
- [11] Hou H, Zhang Y, Li Z, Jiang T, Zhang J and Xu C 2016 Numerical Analysis of Entropy Production on a LNG cryogenic submerged pump *Journal of Natural Gas Science and Engineering* **2016**;36 87–96
- [12] Ameen L M, Kenny R J, Johnson W L and Henkel K L 2024 NASA's Developments in Cryogenic Fluid Management Technology *NASA Technical Report*

- [13] Kenny R J (NASA STMD Cryogenic Fluid Management Portfolio Project Office) 2023 Towards a CFM Flight Demo *NASA Technical Presentation*
- [14] Menéndez-Blanco A, Oro JMF and Meana-Fernández A 2019 Unsteady three-dimensional modeling of the Fluid–Structure Interaction in the check valves of diaphragm volumetric pumps *Journal of Fluids and Structures* **2019;90** 432–49
- [15] Iannetti A, Stickland M T, and Dempster W M 2014 A computational fluid dynamics model to evaluate the inlet stroke performance of a positive displacement reciprocating plunger pump *Journal of Power and Energy* **2014;228** 574–84
- [16] Woo J, Sohn D K, and Ko H S 2020 Analysis of stiffness effect on valve behavior of a reciprocating pump operated by piezoelectric elements *Micromachines* **2020;11** 894.
- [17] Gibson H 2019 Design guide for bearings used in cryogenic turbopumps and test rigs *NASA Technical Report*